

Electrochemical investigations of Al–Mg alloy subjected to tensile test

J. Orlikowski · K. Darowicki

Received: 3 June 2008 / Revised: 28 July 2008 / Accepted: 5 September 2008 / Published online: 23 September 2008
© Springer-Verlag 2008

Abstract Tensile process of Al–Mg alloys exposed to electrochemical environment is accompanied by numerous electrochemical phenomena, the reasons of which depend on both mechanical and electrochemical factors. Identification and description of these phenomena is of fundamental importance. This paper presents the results of impedance investigations carried out during a tensile test of Al–Mg alloys till rupture. The impedance measurements were performed using a dynamic electrochemical impedance spectroscopy (DEIS) technique. It was found that a phenomenon of mechanical cracking of a passive layer occurs in the elastic range, what results in significant breakdown of barrier properties of the layer and thus in an initiation of corrosion processes on the samples' surface. In the plastic range oscillatory changes of electrochemical properties of the samples were identified. The investigations revealed that they were associated with the Portevin–LeChatellier effect. The DEIS measurements were conducted under different electrochemical (various levels of anodic polarization) and mechanical (various strain rates) conditions in order to identify and evaluate the factors influencing a dynamics of changes of electrochemical properties of the alloys.

Keywords Passive layer cracking · DEIS · Tensile stress · PLC effect · Non-stationary signals

Presented at the international conference CORROSION TODAY held in Gdansk-Sobieszewo, Poland, 23 to 26 April 2008

J. Orlikowski (✉) · K. Darowicki
Department of Electrochemistry, Corrosion and Materials
Engineering, Gdańsk University of Technology,
Narutowicza Str. 11/12,
80-952 Gdańsk, Poland
e-mail: juliuszo@plusnet.pl

Introduction

For many years aluminum–magnesium alloys have been the object of numerous scientific researches. They are characterized by very good exploitation properties, among which, the most important are low density and consequent also high strength-to-weight ratio [1–3], good electrical and thermal conductivity [1, 4], good weldability [3, 5], formability and castability [2–3], and high corrosion resistance [3, 5, 6]. Many of these properties depend strongly on magnesium content in the alloy. Good anti-corrosion properties of aluminum–magnesium alloys are due to a passive layer presence. Resistance of the passive layer in different environments and in varying electrochemical conditions has become the subject of many papers [7–10]. Mechanical aspects are important factors influencing on corrosion processes, because mechanical properties of the passive layer have an impact on a kinetics of the stress-corrosion cracking process. Researches involved with the stress-corrosion cracking are well known and widely performed all over the world. Classical stress-corrosion cracking researches are based on electrochemical and mechanical measurements, and metallographical studies [11–12]. A combination of electrochemical and mechanical measurements seems to be an interesting approach aimed at description of mechanical properties of the passive layer. At this point, one must recognize significant measurement obstacles in investigation of Al–Mg alloys resulting from: changes of analyzed surface area, which increases non-linearly during the tensile process and such phenomena as the passive layer cracking as well as the Portevin–LeChatelier (PLC) effect. During plastic deformation of Al–Mg and Al–Cu type alloys it was found that the alloys' surface exhibited some unevenness connected with the serrated yielding phenomenon (the Portevin–LeChatelier

PLC effect). Magnesium or copper atoms are characterized by high mobility in the dissolved state yielding non-uniform plastic strain under typical temperatures and for typical strain rates.

The use of potentiostatic techniques developed the knowledge of the stress-corrosion cracking mechanism [13–15] and allowed the determination of the stress-corrosion cracking characteristic potentials [11–14]. However, these measurements were mainly DC ones, which are ideally suited for investigation of the stationary processes that is when electrochemical properties do not change during the time of measurement. A new approach is execution of electrochemical measurements in dynamic conditions, namely realization of the measurements during the tensile test [16]. In such conditions, the surface area of the samples changes upon their elongation. Thus, DC researches would yield averaged results, which could not be properly interpreted. Classical electrochemical impedance spectroscopy (EIS) also makes possible receiving information, which relate to the stress-corrosion cracking process, but only before and after the moment of cracking, when the investigated system has attained a steady state [17–18]. Basic background of such measurements was widely discussed by Gabrielli [19], Macdonald [20], Mansfeld and Lorenz [21] and Stoynov et al. [22]. However, as for now, detailed determination of the moment of the passive layer cracking in time/strain domain was not possible by means of any electrochemical technique or mechanical test. That is why the methodology of measurement must be changed.

The great evolution of mathematical analyzing techniques enabled to achieve a breakthrough in electrochemical measurements [23–25]. The use of joint time–frequency analysis made possible the analysis of impedance measurements in time or strain domain. This measurement technique allows analysis of mechanism of electrochemical process in time domain including rapid phenomena such as changes in the physical properties of passive films, but it was never used for investigation of dynamic mechanical processes.

Darowicki et al. elaborated a new dynamic impedance technique, which can be very useful in such type of investigation [23–25].

The aim of this work is simultaneous execution of electrochemical (DEIS) and mechanical investigations during the tensile test. They are meant to provide information on an influence of dynamic mechanical factor

(tensile stress) on impedance results. Moreover, the main mechanical and electrochemical factors influencing the obtained characteristics will be identified.

Experimental

Experiments were composed of classical electrochemical DC measurements (cyclic polarization), and AC measurements performed using DEIS.

Detailed electrochemical measurements during the tensile test were conducted for AA5251 aluminum alloy, because it contains relatively small amount of magnesium, which improves both corrosion resistance and plastic properties of the alloy.

Examined samples were made in the form of bars according to the ASTM standard. Detailed chemical composition of investigated AA5251 aluminum alloy based on the UNS Number (Unified Numbering System for Metals and Alloys) is presented in Table 1.

The samples were mounted in a measurement cell and then in a tensile testing machine MTS 81012. Tensile tests and samples preparations were performed according to EN 10002-1 +AC1 standard at room temperature with the MTS extensometer characterized by the measurement base of 40 mm. The mechanical investigations consisted in tensile tests of the samples carried out until their rupture with simultaneous stress/strain recording. The strain changed linearly versus time and the applied strain rates were as follows: $d\varepsilon/dt=1\times 10^{-2}\text{ s}^{-1}$, $5\times 10^3\text{ s}^{-1}$, $1\times 10^3\text{ s}^{-1}$, $5\times 10^4\text{ s}^{-1}$.

The electrochemical measurements were performed simultaneously with the mechanical ones. Examinations were carried out in a three-electrode electrochemical cell, in which silver/silver chloride electrode was used as a reference electrode and an auxiliary electrode was made of platinum net.

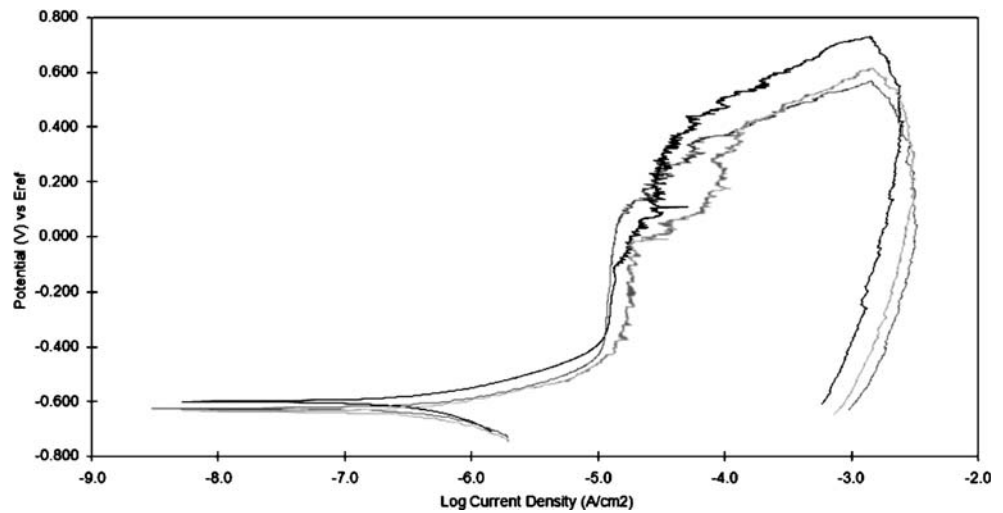
The electrochemical measurements were conducted in buffered solution ($\text{H}_3\text{BO}_3+\text{Na}_3\text{BO}_3$; $\text{pH}=7.4$) with additional content of 0.002 M sodium chloride. The geometrical area of examined samples was equal to 19.6 mm^2 .

Additionally, the electrochemical examinations were carried out under tensile stresses in such a way that a time of the DEIS measurements was correlated with the strain process. The measurement was stopped when the sample was broken. Average recorded strain value for AA5251 was of 18% (0.18). A basic measurement set-up consisted of electrochemical measurement software Gamry International.

Table 1 Chemical composition of investigated AA5251 alloy (atomic %)

Mg	Zn	Cr	Fe	Mn	Cu	Other
1.7–2.4	–	Max 0.15	Max 0.4	0.01–0.05	Max 0.15	Bal

Fig. 1 A series of exemplary graphs showing the results of potentiodynamic measurements performed on AA5251 alloy in buffer solution



Rate of potential changes was 1 mV^{-1} . The DEIS measurements were realized using KGLstat v. 2.1 potentiostat and a National Instruments PCI 6120 card generating the perturbation signal, registering voltage perturbation and current response signals. Impedance measurements were executed for the frequency range: 20 kHz–3 Hz. The average number of points per decade in the DEIS measurements was 5. A sampling frequency of 100 kHz resulted from the measurement card settings being at our disposal. In the investigations the multi-sinusoidal signal composed of 20 sinusoids was utilized. Depending on applied frequency, the amplitudes of sinusoidal signals were ranging from 3 to 18 mV. The papers [24, 25] contain detailed description of this method.

Results and discussion

Prior to execution of simultaneous electrochemical and mechanical measurements it was necessary to evaluate basic electrochemical properties of AA5251 alloy exposed to borate solution with additional content of 2 mM sodium chloride. That is why potentiodynamic cyclic polarization tests were performed and their results are presented in Fig. 1.

A series of 20 samples prepared in an identical way were investigated in order to determine the passive range and pitting corrosion potential of the alloy. Obtained results were subjected to elementary statistical evaluation. The stationary potential was equal to $-0.630 \pm 0.020 \text{ V}$

and the pitting corrosion potential at current density of $5 \times 10^4 \text{ A/cm}^2$ was $-0.180 \pm 0.022 \text{ V}$. Accordingly, it can be seen that the passive range is relatively broad in the investigated environment.

Before the main experiment, a series of mechanical tests were also carried out aimed at determination of fundamental mechanical parameters. They consisted in the tensile tests performed for various strain rates from $d\varepsilon/dt=5 \times 10^4 \text{ s}^{-1}$ to $d\varepsilon/dt=1 \times 10^2 \text{ s}^{-1}$. Table 2 gathers characteristics of the fundamental mechanical parameters of AA5251 alloy.

Figure 2 depicts an exemplary stress–strain curve and potential–strain plot obtained for the strain rate $d\varepsilon/dt=5 \times 10^3 \text{ s}^{-1}$.

The stress–strain curve of AA5251 alloy (Fig. 2a) exhibits certain oscillations. This phenomenon is termed the Portevin–LeChatelier (PLC) effect. During the plastic treatment, irregularity of surface, or what is known as the serrated yielding phenomenon or the Portevin–LeChatellier effect (PLC), appears [26]. Very thorough mathematic analysis was conducted by Hähner and some other scientists [27–29]. The discussed phenomenon concerns aluminum alloys containing magnesium. Magnesium molecules are characterized by high mobility in liquid phase, which causes unequal process of plastic deformation under typical temperatures and strain rates. Research of serration process was conducted with many aspects taken into consideration.

Very often, during realization of tensile process of Al–Mg alloys, many types of serration occur which makes it very difficult to define dynamic parameters. The group of

Table 2 Mean values of mechanical parameters obtained on the basis of a series of tensile tests

Min proof stress 0.2%	Proof stress 0.2%	Min ultimate tensile strength	Ultimate tensile strength	Hardness, Brinell	Hardness, Vickers
130 MPa	175 MPa	205 MPa	215 MPa	65	70

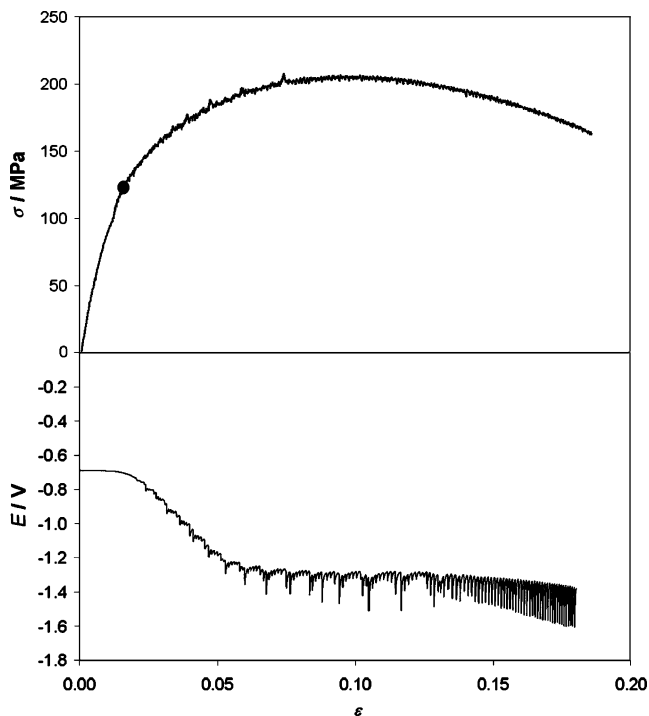


Fig. 2 An exemplary stress–strain curve for AA5251 alloy (a) and stationary potential plot (b) recorded for the strain rate $d\varepsilon/dt=5\times 10^3\text{ s}^{-1}$

Al–Mg alloys is characterized by two types of serration: A and B [30]. Type A is characterized by perturbations on stress–strain curve in the form of many peaks, which occur with variable regularity as a function of strain. On the other hand, type B describes irregular stress changes as a function of strain.

Observed oscillations are the effect of non-uniform changes of surface area of the sample subjected to tensile process. Simultaneous electrochemical and mechanical investigations revealed that anodic polarization has no influence on mechanical parameters. For the highest anodic potentials, a process of electrode dissolution lasts too short to have any impact on the mechanical properties of the investigated material. Strain rate in the range from $d\varepsilon/dt=1\times 10^2$ to $5\times 10^4\text{ s}^{-1}$ influences only on an intensity of the PLC effect [30]. Basic mechanical properties do not change significantly for this range of strain rate.

Figure 2b shows also very dynamic changes, which occur on a surface of the investigated sample. One can notice a significant drop of potential versus strain as well as some oscillations of various frequencies. At the beginning of the tensile test, the potential is constant and it takes the same value as in the case of non-strained samples. Until the strain $\varepsilon=0.02$ is reached, there are no oscillations and no significant fluctuations of potential. Beyond $\varepsilon=0.02$, a rapid drop of potential is observed, whereas for the strain values higher than $\varepsilon=0.03$, a decrease in potential is accompanied by its irregular oscillations. These oscillations

become more regular for the strain beyond $\varepsilon=0.06$. For the strain values following $\varepsilon=0.08$ the mean value of potential does not decrease and is equal to -1.3 V . For $\varepsilon=0.13$, the oscillations of potential change their character, while the mean value of potential decreases slightly down to -1.4 V , just before the rupture. A preliminary analysis suggests proceeding of very complicated processes, which have an influence on electrochemical properties of surface of the investigated material. A significant decrease in potential observed since $\varepsilon=0.02$ indicates cracking of the passive layer due to increasing strain. Detailed researches on alloy steels and aluminum alloys revealed that passive layer cracking occurs for defined values of strain [16, 32–34]. A value of the critical strain, for which the passive layer cracks can be precisely determined for a given alloy using the DEIS and acoustic emission methods [35]. Regular oscillations of potential recorded during the tensile test are connected with the PLC effect. Non-uniform process of change of surface area of the specimen results in significant fluctuations of potential.

In order to relate the recorded mechanical parameters (Fig. 2a) to the electrochemical results (Fig. 2b), a time–frequency analysis of the stress records was performed with the short-time Fourier transformation employing Hanning window [31]. The exemplary results of such analysis, carried out for the strain rate $d\varepsilon/dt=5\times 10^3\text{ s}^{-1}$, are shown in Fig. 3.

The obtained spectrogram reveals presence of several frequency bands, which are connected with the PLC effect of type A and B. For the strain higher than $\varepsilon=0.15$, there is only type B serration, which is characterized by a few harmonic bands; the lowest band has the frequency $f=0.6\text{ Hz}$. Applied mathematical analysis allowed description of a character of the oscillations in the strain domain (measurement time is proportional to strain).

The oscillations of potential (Fig. 2b) suggest implementation of the same analysis as in the case of mechanical investigations. Accordingly, the time–frequency analysis with the short-time Fourier transformation employing

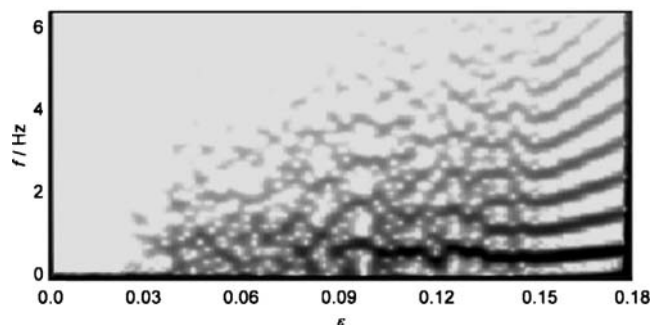


Fig. 3 A frequency–strain plot for the strain rate $d\varepsilon/dt=5\times 10^3\text{ s}^{-1}$, obtained as a result of analysis using the short-time Fourier transformation with Hanning window

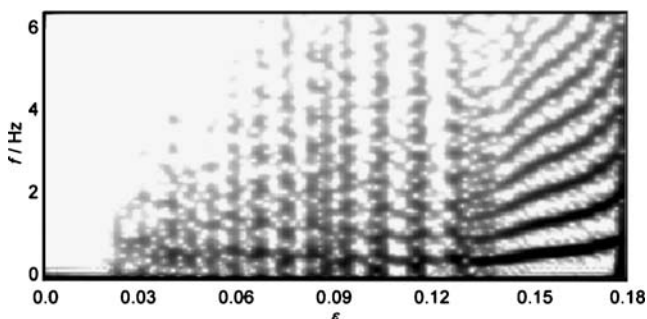


Fig. 4 A frequency–strain plot for the stationary potential record obtained during the tensile test of AA5251 alloy ($d\varepsilon/dt=5 \times 10^3 \text{ s}^{-1}$); analysis using the short-time Fourier transformation with Hanning window

Hanning window was performed and an exemplary resultant spectrogram is depicted in Fig. 4.

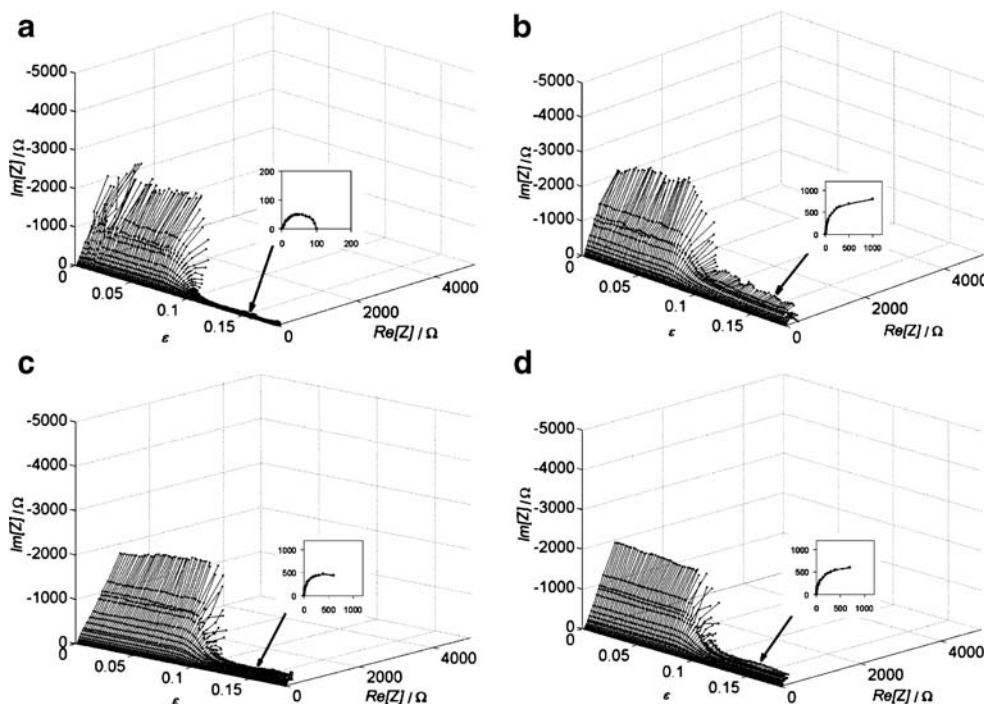
High conformity can be seen while comparing both spectrograms (Figs. 3 and 4), which are based on the analysis of strain and potential respectively. It means that the PLC effect causes changes of surface area what can be detected by potential measurements. Instantaneous increase in the active surface area is accompanied by a decrease in potential, which represents an image of irregular changes of surface. The decrease in potential is connected with exposure of the active surface area, not covered with any oxide layers. An increase in potential corresponds to a stage of the tensile process, during which change of the active surface area is minimum. An intention of application of the buffer solution in the studies was to avoid active dissolution of aluminum during dynamic changes of surface area of the

strained samples. In case of both spectrograms, the frequencies of particular harmonic bands of the type B serration are close to each other. Certain differences arise when assessing presence of the type A and type B serration in the strain range from $\varepsilon=0.03$ to $\varepsilon=0.14$. The PLC effect exhibits much higher regularity (well-resolved bands localized in the time domain) in the case of potential measurement results (Fig. 4) than on the spectrogram corresponding to the analysis of stress versus strain (Fig. 3). Performed comparative analysis clearly showed that the measurement of potential of the electrode subjected to the tensile process was consistent with the mechanical characteristic. So, this method can be applied for an analysis of the surface PLC effect. Thus, it is possible to correlate mechanical changes with the changes of the surface area subjected to electrochemical measurements.

The next stage of investigation consisted in dynamic electrochemical impedance spectroscopy measurements during the tensile test. The measurements were carried out in a potentiostatic mode for different levels of anodic polarization as well as for different strain rates at constant potential. Such approach enables evaluation of an influence of both electrochemical and mechanical factors on kinetics of the electrochemical processes occurring during the tensile process.

Figure 5 presents the impedantiograms from the DEIS measurements conducted for the following levels of anodic polarization $E=-0.390, -0.460 \text{ V}$ and for the strain rate $d\varepsilon/dt=5 \times 10^3 \text{ s}^{-1}$ (Fig. 5a,b). Figure 5c and d illustrate the impedantiograms from the DEIS measurements conducted

Fig. 5 DEIS spectrograms recorded during the tensile test of examined AA5251 aluminum alloy: at potentials **a** $E=-0.390 \text{ V}$, **b** $E=-0.460 \text{ V}$ for the strain rate $d\varepsilon/dt=5 \times 10^3 \text{ s}^{-1}$ as well as at potential $E=-0.430 \text{ V}$ for the strain rates **c** $d\varepsilon/dt=5 \times 10^3 \text{ s}^{-1}$ and **d** $d\varepsilon/dt=5 \times 10^4 \text{ s}^{-1}$



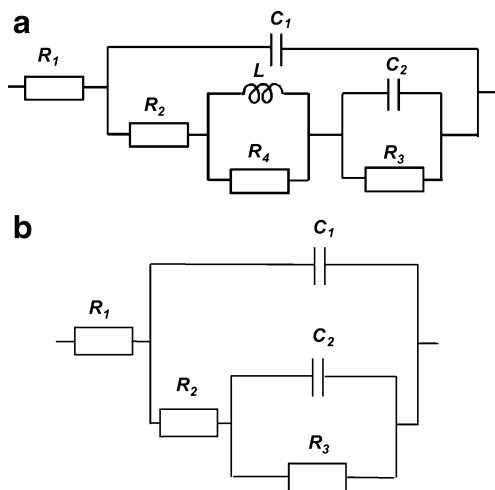


Fig. 6 Original (a) and applied (b) equivalent circuits used in electrochemical analysis of impedance spectra recorded for AA5251 aluminum alloy

for the anodic polarization $E = -0.430$ V and for the strain rates $d\varepsilon/dt = 5 \times 10^3$ s⁻¹ and $d\varepsilon/dt = 5 \times 10^4$ s⁻¹, respectively.

Presented DEIS impedantiograms show a significant change of impedance during the tensile test. In each case,

there is a rapid change of impedance beyond $\varepsilon = 0.05$. Capacitive character of the spectra (almost straight lines) changes into the form suggesting an activation control of the process (spectra in the form of semicircles). The capacitive character is very similar in case of all the spectra. In this strain range, a stable passive state can be observed; changes occur for higher strain values. From the DEIS measurements it is evident that for higher levels of polarization the size of the impedance semicircles (for high strain values) decreases with an increase in anodic polarization (Fig. 5a and b). It indicates cracking of the passive layer and the influence of anodic polarization level on kinetics of dissolution of the investigated alloy. Similar conclusions can be drawn when the strain rate is a variable parameter. For higher strain rates, a dynamics of surface area change is higher and, accordingly, the kinetics of electrochemical processes increases (Fig. 5c and d). Anodic polarization and strain rate do not have an influence on the passive range, which is observed up to $\varepsilon = 0.05$. Equivalent circuit proposed by Lee [36], Bessone et al. [37] and Brett et al. [38] has been employed in Fig. 6a. Some parameters presented in Fig. 6a should be defined: R_1 —the electrolyte resistance, R_2 —the resistance of internal sublayer of

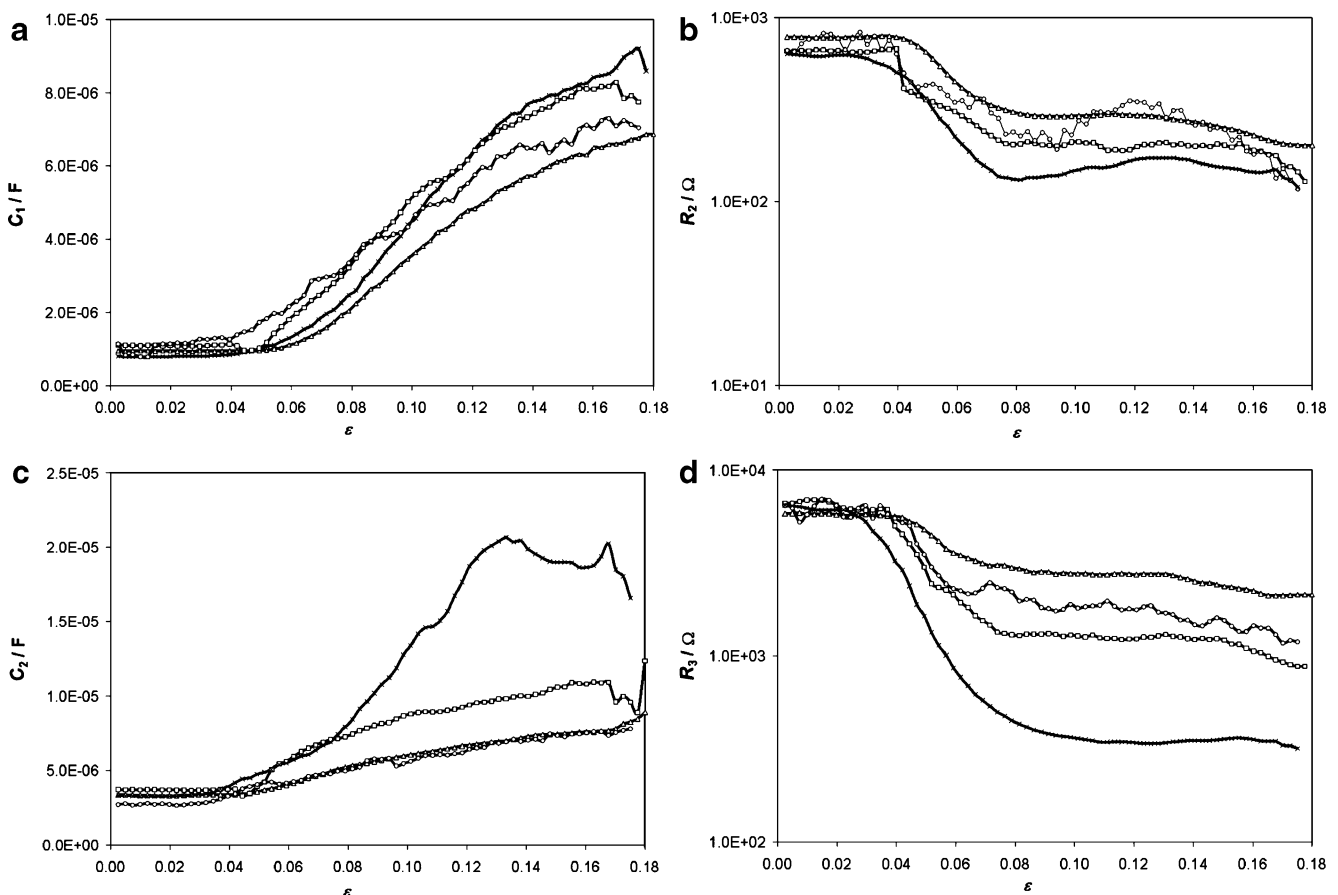


Fig. 7 Electrochemical parameters of AA5251 alloy received on the basis of employed equivalent circuit versus strain under various potential conditions: $E = x$ symbol -0.390 V, open circle -0.430 V, open square -0.460 V, open upright triangle -0.525 V for the strain rate $d\varepsilon/dt = 5 \times 10^3$ s⁻¹

examined passive film/resistance of porous passive film in the active state, C_1 —the capacitance of internal sublayer of examined passive film/capacitance of porous passive film in the active state, R_3 —the resistance of external sublayer of examined passive film/charge transfer resistance in the active state, C_2 —the capacitance of external sublayer of examined passive film/double layer capacitance in the active state, R_4 —the adsorption resistance of transition product; L , inductance. However, the calculation of R_4 and L was not possible because of applied frequency range, these parameters can be determined only for low frequencies. Therefore, the employed equivalent circuit was simplified in the form illustrated in Fig. 6b.

Figure 7a–d shows the dependencies between particular parameters of the equivalent circuit and strain for different levels of anodic polarization $E = -0.390, -0.430, -0.460, -0.520$ V and for the strain rate $d\varepsilon/dt = 5 \times 10^3 \text{ s}^{-1}$.

The changes of particular electrical parameters reveal certain characteristic regularity. Up to the strain value $\varepsilon = 0.02\text{--}0.04$, all the parameters are stable, it means they do not depend on strain. The values of resistances R_2 and R_3 are high, which confirms the presence of a tight oxide layer and stable passive state. Above $\varepsilon = 0.02\text{--}0.04$, there is a

significant dynamics of changes, reflected in big differences in impedance (Fig. 7). Resistance of both sublayers R_2 and R_3 decreases due to cracking of the passive layer. Capacitances C_1 and C_2 also change. Beyond $\varepsilon = 0.04$ they both increase, most probably because of water absorption. It confirms the hypothesis about mechanical cracking of the passive layer. Significant differentiation of the parameters as a function of anodic polarization potential is detected for higher values of strain. It is especially clear for the resistance R_3 (Fig. 7d). In the active state, which is for the strain higher than $\varepsilon = 0.02\text{--}0.04$, this parameter describes charge transfer resistance. So, for higher values of anodic polarization, there is bigger decrease in R_3 . For significant strain $\varepsilon > 0.10$, the resistance R_3 does not undergo dynamic changes.

Figure 8a–d presents the dependencies between particular parameters of the equivalent circuit and strain for the anodic polarization $E = -0.430$ V and for the following strain rates $d\varepsilon/dt = 1 \times 10^2 \text{ s}^{-1}, 5 \times 10^3 \text{ s}^{-1}, 1 \times 10^3 \text{ s}^{-1}, 5 \times 10^4 \text{ s}^{-1}$.

The characteristics presented in Fig. 8 enable evaluation of the influence of different strain rate on the electrochemical processes proceeding on a surface of the samples subjected to the tensile test. The magnitudes of particular

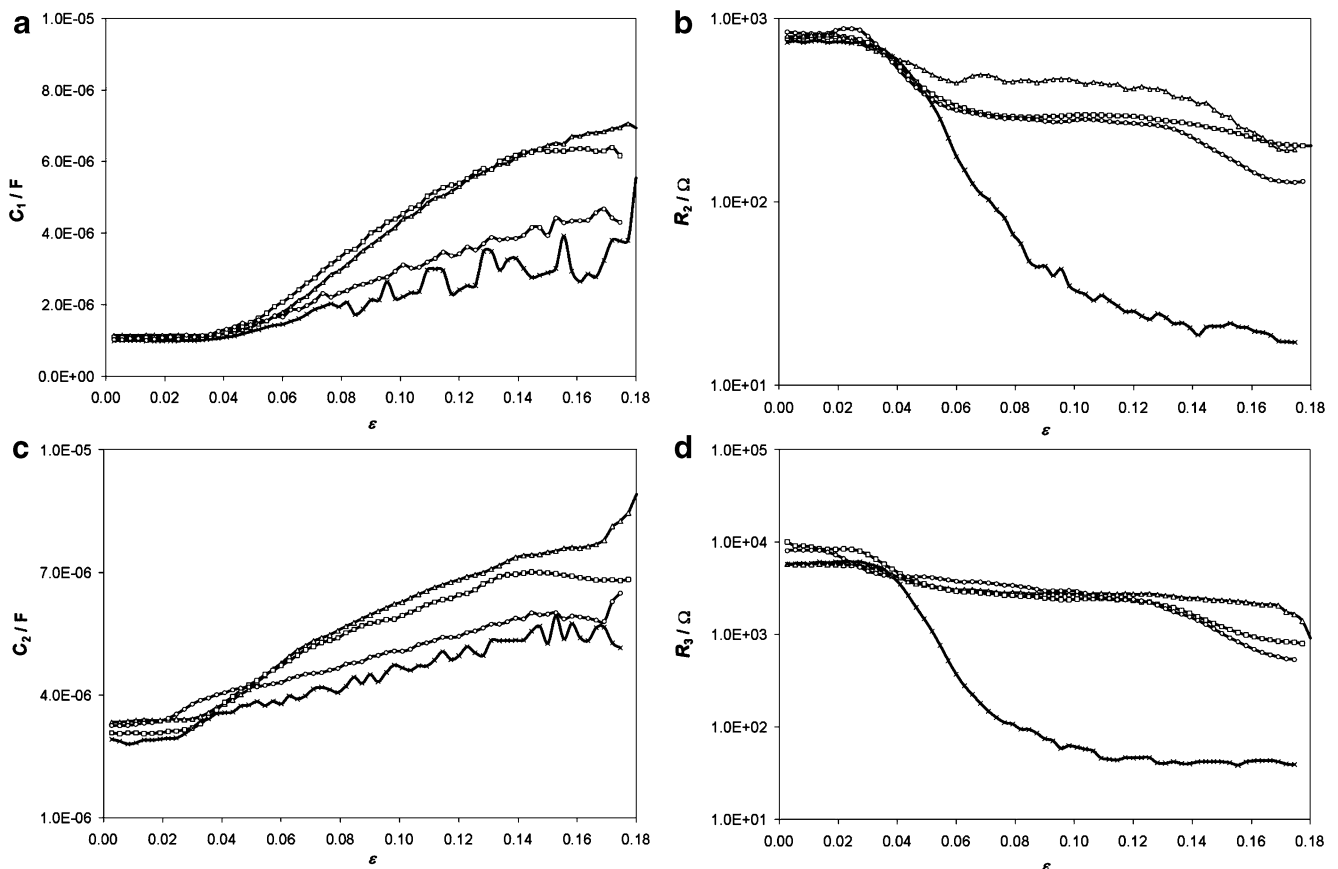


Fig. 8 Electrochemical parameters of AA5251 alloy received on the basis of employed equivalent circuit versus strain for various strain rates: $d\varepsilon/dt = x$ symbol $1 \times 10^2 \text{ s}^{-1}$, open circle $5 \times 10^3 \text{ s}^{-1}$, open square $1 \times 10^3 \text{ s}^{-1}$, open upright triangle $5 \times 10^4 \text{ s}^{-1}$ for the potential $E = -0.430$ V

electrical parameters and dynamics of their changes are comparable to the ones presented previously (Fig. 7). Cracking of the passive layer occurs for the strain higher than $\varepsilon=0.02$ – 0.04 , just in the previous cases. In the active range, an increase in the strain rate has a similar impact on electrochemical process as the increase in anodic polarization.

Based on the performed measurements some discrepancies can be noticed as far as evaluation of the critical strain is concerned, for which passive layer cracking was observed. According to the stationary potential measurements (Fig. 2b) and to the resistance R_3 course (Figs. 7d and 8d), this critical strain was equal to $\varepsilon=0.02$. Based on evolution of the remaining parameters, cracking of the passive layer occurred for $\varepsilon=0.04$. Such difference in the critical strain value should be interpreted as a delay in an initiation of the electrochemical processes of aluminum dissolution. Detailed analysis of this problem has been presented in the previous paper [35].

The critical value of strain $\varepsilon=0.02$, for which cracking of the passive layer was detected (based on stationary potential measurements and resistance R_3 analysis), was overlapped with the stress–strain curve presented in Fig. 2a (indicated with a circle on the plot). It is evident that passive layer cracking occurs in the elastic range. Thus, it is likely that passive layer cracking will appear in the range of exploitation loads, what as a consequence can result in stress-corrosion cracking of the material.

Conclusions

Combined electrochemical and mechanical investigations allow stating the following conclusions:

- Tensile process and simultaneous exposure to an electrochemical environment result in significant changes of surface state of the samples.
- A stable passive state is observed at the beginning of the tensile test. The values of electrochemical parameters do not depend on the level of anodic polarization and on the strain rate.
- Analysis of the electrochemical properties based on the potential measurements and DEIS investigations revealed that mechanical damage of the passive layer occurs for the strain value lying within the elastic range.
- After the passive layer cracking, on the active surface there proceed some electrochemical processes, the rate of which depends on the level of anodic polarization as well as on the strain rate.
- An influence of the PLC effect on the electrochemical properties was observed in the plastic range. There exists a correlation between frequency characteristic of the registered potential and magnitude of strain.

Instantaneous change of surface area, due to the PLC effect, has an impact on changes of potential.

- Proposed methodology is a new approach to analysis of complex electrochemical phenomena, which occur during the tensile process.

Acknowledgment The contribution has been realized as a part of the grant 3 T08C 001 30 financed by the Ministry of Science and Higher Education.

References

1. Singh P, Suryanarayana C (2003) *Intermetallics* 11:373
2. Jiang DM, Wang CL, Yu J, Gao ZZ, Shao YT, Hu ZM (2003) *Scr Mater* 49:387
3. Palasantzas G, Van Agterveld DTL, De Hosson JTM (2002) *Appl Surf Sci* 191:266
4. Shuaib AN (2002) *Mater Des* 23:181
5. Brillas E, Cabot PT, Centellas F, Garrido JA, Perez E, Rodriguez RM (1998) *Electrochim Acta* 43:799
6. Griguzeviciene A, Leinartas K, Juskenas R, Juzeliunas E (2004) *J Electroanal Chem* 565:203
7. Blanc C, Freulon A, Lafont MC, Kihn Y, Mankowski G (2006) *Corros Sci* 48:3838
8. Martin FJ, Cheek GT, O'Grady WE, Natishan PM (2005) *Corros Sci* 47:3187
9. Hashimoto K, Asami K, Kawashima A, Habazaki H, Akiyama E (2007) *Corros Sci* 49:42
10. Armstrong RD, Braham VJ (1996) *Corros Sci* 38:1463
11. Garcia C, Martin F, De Riedra P Heredero J, Aparicio M (2001) *Corros Sci* 43:1519
12. Loria A (1982) *J Met* 34:16
13. Haruna T, Shibata T, Toyota R (1997) *Corros Sci* 39:1935
14. Kolamn D, Ford D, Butt D, Nelson T (1997) *Corros Sci* 39:2067
15. Cihal V, Stefec R (2001) *Electrochim Acta* 46:3867
16. Darowicki K, Orlikowski J, Arutunow A (2003) *Electrochim Acta* 48:4189
17. Identification of electrochemical processes by frequency response analysis (1995) Cohen L, Technical Report Number 004/83, Farnborough
18. Techniques for Characterization of Electrodes and Electrochemical Processes (1991) In: Macdonald DD (eds) Varma R, Selman JR, 515, Wiley, NY
19. Use and Applications of Electrochemical Impedance Spectroscopy (1990) Gabrielli C, Technical Report, Ch.II, Schlumberger Technologies, Farnborough
20. Impedance Spectroscopy (1987) (eds) Macdonald JR, Wiley, NY
21. Techniques for Characterization of Electrodes and Electrochemical Processes (1991) In: Mansfeld F, Lorenz WJ (eds) Varma R, Selman JR, 581, Wiley, NY
22. Electrochemical Impedance (1991) Stoinov B, Grafov BM, Savova-Stoinova B, Elkin WW, Nauka, Moscow
23. Darowicki K (2000) *J Electroanal Chem* 486:101
24. Darowicki K, Lentka G, Orlikowski J (2000) *J Electroanal Chem* 486:106
25. Darowicki K, Slepski P (2003) *J Electroanal Chem* 547:1
26. Portevin A, LeChatellier F (1923) *Compte Rend Acad Sci Paris* 176:507
27. Hähner P (1993) *Mater Sci Eng A* 164:23

28. Ziegenbein A, Hähner P, Neuhauser H (2000) *Comp Mater Sci* 19:27
29. Hähner P (1997) *Acta Mater* 45:3695
30. Wen W, Zhao Y (2005) *Mater Sci Eng A* 392:136
31. *Time–frequency analysis* (1995) Cohen L, Prentice Hall, NY
32. Darowicki K, Orlikowski J, Arutunow A (2004) *J Solid State Electrochem* 8:352
33. Darowicki K, Orlikowski J, Arutunow A (2004) *Corros Eng Sci Tech* 39:255
34. Darowicki K, Orlikowski J, Arutunow A, Jurczak W (2005) *Electrochem Solid-State Lett* 8:B55
35. Darowicki K, Orlikowski J, Arutunow A, Jurczak W (2007) *J Electrochem Soc* 154:74
36. Lee EJ, Pyun SJ (1995) *Corros Sci* 37:157
37. Bessone JB, Salinas DR, Mayer CE, Ebert M, Lorenz WJ (1992) *Electrochim Acta* 12:2283
38. Brett CMA, Gomes IAR, Martins JPS (1994) *J Appl Electrochem* 24:1158